Preparation of a Ribonucleic Acid–(Polyamidoamine)–(Zirconia–Urea-Formaldehyde Resin) High-Performance Liquid Affinity Chromatographic Stationary Phase

Shulei Lei, Shilin Yu*, and **Chunfeng Zhao**

College of Science, Beijing University of Chemical Technology, 15 Beisanhuan East Road, Chaoyang District, Beijing 100029, China

Abstract

A preparative method for a high-performance liquid affinity chromatographic (HPLAC) stationary phase is described. The 3- to 5-µm nonporous composite spherical microparticles of zirconia and urea-formaldehyde (UF) resin are synthesized through the reaction of zirconyl chloride with hexamethylene tetra-amine and urea, and then it is used as the matrix of the HPLAC stationary phase of which the diameter and structure are determined by scanning electron microscopy. In a methanol medium, the polyamidoamine (PAMAM) starburst dentritic spacer arms are linked with the imido-groups on the surface of the matrix by the Michael addition reaction with methyl acrylate and the amination reaction with ethylene diamine. After repeating these steps in triplets, amine-terminated dentritic spacer arms with a generation of 3 are obtained. The topological structure of the spacer arms is examined by solid-state ^{13}C NMR. The Br-substituted ribonucleic acid (RNA) ligand is obtained by the reaction of liquid bromine with RNA and bonded to the dendritic spacer arms of the matrix in a solution of NaOH (pH 9–11). The binding capacity of RNA is measured by UV spectrophotometry. A new type of stationary phase—RNA–(PAMAM)–(zirconia–UF resin—for HPLAC, which possesses starburst dendritic spacer arms, is synthesized and used for the separation of biological macromolecules.

Introduction

In pace with the rapid development of bioengineering techniques, molecular biology, and pharmaceutical molecular design, high-performance liquid affinity chromatography (HPLAC) has been increasingly used for the separation of biological macromolecules (1–4). A common feature of biological macromolecules is their ability to recognize and bind to other molecules, often in a highly specific manner. It is this specific biological recognition and selective binding ability that allows all biological macromolecules to be separated and purified by HPLAC. These macromolecules are generally separated by using columns that are packed with a macroporous (30–100 nm) rigid microparticulate (10–30 µm) such as SiO_2 or polystyrene beads (5). However, a low diffusivity of biological macromolecules and limited mass transfer in the pores of the column packing often result in a long retention time, low recovery rate of mass, and loss of biological activity, thus showing poor chromatographic performance.

Therefore, many attempts have been undertaken to use a nonporous rigid microsphere matrix for separating biological macromolecules (6–14). The nonporous packings lack intraparticle pores. This allows for the maintaining of a better mass transfer, shorter retention time, higher bioactivity, and recovery rate of biomacromolecules. However, nonporous packings have two obvious limitations (i.e., small column capacity for a low surface area of a nonporous microsphere and high column pressure drop for a small diameter of matrix).

In order to overcome the shortcomings of a nonporous microsphere, a shorter column is used to reduce the column pressure drop and obtain high column efficiency. In addition, the starburst dendritic spacer arms are coupled with the external surface of the nonporous microsphere matrix for the sake of enlarging the column capacity.

The starburst dendritic spacer arms differ from the linear spacer arms because of their extraordinary symmetry, high branching, and maximum terminal density of the functional group. Consequently, when the ligands are bonded to terminal function groups of starburst dendritic spacer arms, the capacity of ligand and column capacity are remarkably increased.

In this study, a new type of stationary phase coupled with starburst dendritic spacer arms of HPLAC is described. The 3- to 5-µm nonporous composite microspheres of zirconia and urea-formaldehyde (UF) resin are used as the matrix of the HPLAC stationary phase, and amine-terminated polyamidoamine (PAMAM) starburst dendritic spacer arms are coupled with the imido groups on the surface of the matrix. Finally, the ribonucleic acid (RNA) brominated ligands with molecular recognition and selective binding are bonded to the amine-terminated groups of the starburst dendritic spacer arms. This HPLAC stationary phase can be

*Author to whom correspondence should be addressed.

used for rapid and high-effective separation of biological macromolecules.

Experimental

Apparatus and reagents

An LC-6A high-performance liquid chromatograph (UVD) (Shimadzu, Tokyo, Japan), a 124A slurry column packer (Chemco, Tokyo, Japan), an S250 MK3 scanning electron microscope (Cambridge Instruments Ltd., Cambridge, U.K.), an AM300 solid-state nuclear magnetic resonance (NMR) apparatus (Bruker, Rheinstetten, Germany), and a UV–vis spectrophotometer (Specord, Beijing, China) were used.

Zirconyl chloride, sodium acetate, sodium hydroxide, sodium dihydrogen phosphate, sodium hydrogen phosphate, hydrochloric acid, hexamethylene tetra-amine (HMTA), urea, heptane, Span 80, Span 85, Tween 80, methyl acrylate (MA), ethylene diamine (EDA), liquid bromine, methanol, ethanol, acetone, propanol, carbon tetrachloride, isopropanol, acetonitrile, thihydroxymethylaminomethane-HCl, and *N*-2-hydroxyethylpiperazine-*N*'-2-ethane sulfonic acid were used as reagents. All of these reagents were analytically pure and made in a Beijing chemical reagent factory. The biological reagents used were adenosine monophosphate (AMP), adenosine diphasphate (ADP), adenosine triphosphate (ATP), bovine serum albumin, Cytochrome C, and cellulases. All of the biological reagents were from the Shanghai Institute of Biological Chemistry. RNA was obtained from Torula yeast (Sigma).

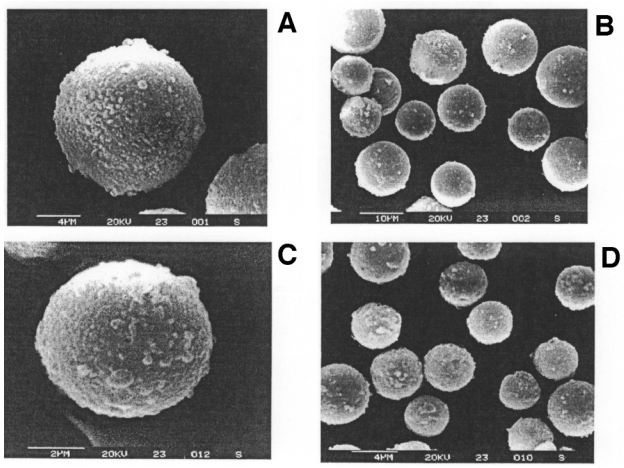

Figure 1. Photographs from a scanning electron microscope of zirconia and UF resin composite: (A) 15-µm composite microspheres, (B) 10–12-µm composite microspheres, (C) 7-µm composite microspheres, and (D) 3–5-µm composite microspheres.

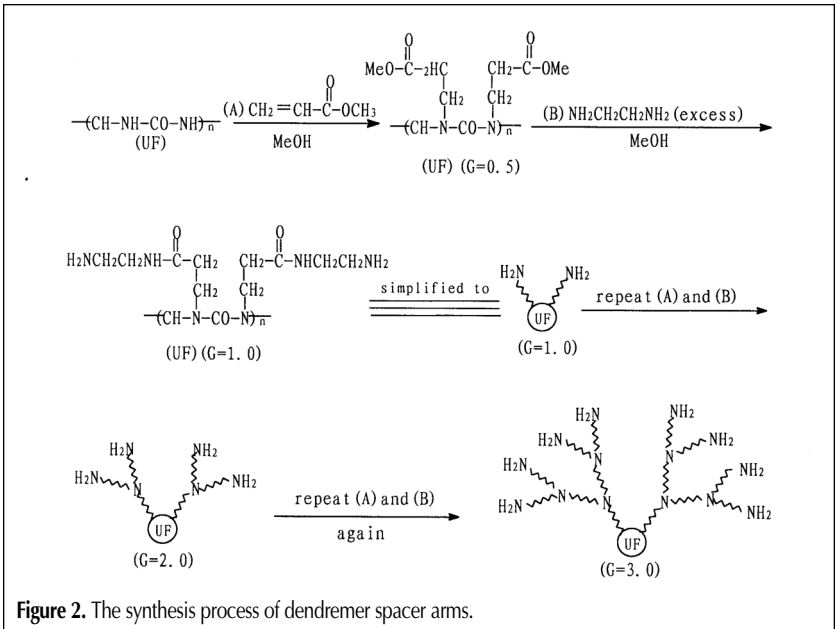

Figure 2. The synthesis process of dendremer spacer arms.

Preparation of the composite microspheres of zirconia and UF resin as a matrix of HPLAC stationary phase

A typical preparation was carried out by the following procedure (15). In a flask with a magnetic stirrer, a multiemulsifer complex was added. The complex contained 5.0 g Span 85, 5.0 g Span 80, 0.5 g Tween 80, and 200 mL heptane and formed the organic phase (oil phase). Then, a certain amount of 2.35-mol/L zirconyl chloride solution (water phase) was slowly added to the oil phase. Consequently, a W/O emulsion that was finely dispersed was formed by using a magnetic stirrer. After stirring for 15 min, a certain amount of a 3.5-mol/L HMTA and a 8.0-mol/L urea mixture solution was dropwise-added into the emulsion within 2 min at a slower stirring velocity. When sufficient hydroxyl ions were released owing to the hydrolysis of HMTA and urea, the homogeneous, rigid, and porous zirconia gels were obtained.

After the total mixture solution of HMTA and urea was quickly added to the emulsion, the stirring velocity was rapidly increased and maintained for 10 min. In the meantime, the UF resin was formed through the condensation reaction of urea and formaldehyde that was produced by the hydrolysis of HMTA. Therefore, the resin was packed into the pores of the porous zirconia. The temperature during the whole process was kept at 50°C. As a result, the nonporous composite particulate hydrogel of zirconia and UF resin was obtained. When the stirring was stopped, the oil phase of the upper layer of the reaction liquid was removed. The composite hydrogel was washed with acetone. During this time the composite hydrogel was converted into white solid microparticulate. The product was washed with acetone, ethanol, and deionized water for 1–3 times. Finally, the composite microspheres were immersed in ammonia water for 24 h and then washed with deionized water until neutrality, followed by drying at 40°C. In Figure 1 are the photographs from a scanning electron microscope of zirconia and UF resin composite microspheres.

Coupling of starburst dendritic spacer arms

The PAMAM dendrimer is one of the first families of dendrimers that has been synthesized and characterized in great detail (16–18).

The starburst dendrimers of PAMAM are synthesized by a two-step reaction process. The first step is an exhaustive Michael addition of a suitable

amine initiator core with MA, and the second step is an exhaustive amidation of the resulting esters with large excesses of EDA.

The completion of this two-step process gives a full generation (G = 1.0); if only one step is finished, then half generation (G = 0.5) is obtained. Repeating this two-step reaction sequence together with purification at each step leads to second (G = 2.0) and third generation (G = 3.0), depending on the numbers of repetition.

The starburst dendritic spacer arms differed from the classical random coil linear spacer arms and were highly branched into a three-dimensional radiator with a large number of active end groups. Moreover, these active end groups easily reacted with many reagents to produce new dendrimers with various functional groups on the surface.

A typical reaction process in which PAMAM starburst dendritic spacer arms are coupled with the zirconia and UF resin composite microsphere matrix was performed in the following method (the reaction process is shown in Figure 2).

First, an appropriate amount of composite microsphere matrix was mixed with MA and methanol and reacted for 12.5 h at 25°C to 30°C by means of a magnetic stirrer. The molar ratio of the amido groups on the surface of the matrix to MA was 1:280. Second, after Michael addition reaction was completed, the reaction product (G = 0.5) was washed 3–4 times with methanol, followed by drying at 47°C in vacuo to remove excess MA and methanol. Then, the dried reaction product (G = 0.5) was blended with EDA and methanol and reacted for 19.5 h at 40°C while stirring in order to complete the amidation reaction and give a full generation. The final product (G = 1.0) was also washed and dried as previously described. Repetition of this two-step reaction could lead to second and third generation. Consequently, the activated composite microsphere matrix was obtained by coupling starburst dendritic spacer arms with a large number of amine active end groups.

The amounts of reactant and reagent in the synthetic process of the PAMAM starburst dendritic spacer arms are given in Table I.

Table I. Amount of Reactant and Reagent in the Synthetic Process of the Dendritical Spacer Arms

G	Weight of reactant (g)	Volume of MA added (mL)	-NH– and MA molar ratio	Volume of EDA added (mL)	-NH– and ED molar ratio	Reaction time (h)
0.0	5.0075	84	1:280			
12.5						
0.5	4.6427			130	1:590	19.5
1.0	4.2760	125	1:420			19.5
1.5	3.2855			175	1:795	18.0
2.0	3.2395	200	1:670			18.5
2.5	2.9811			300	1:1361	22.0

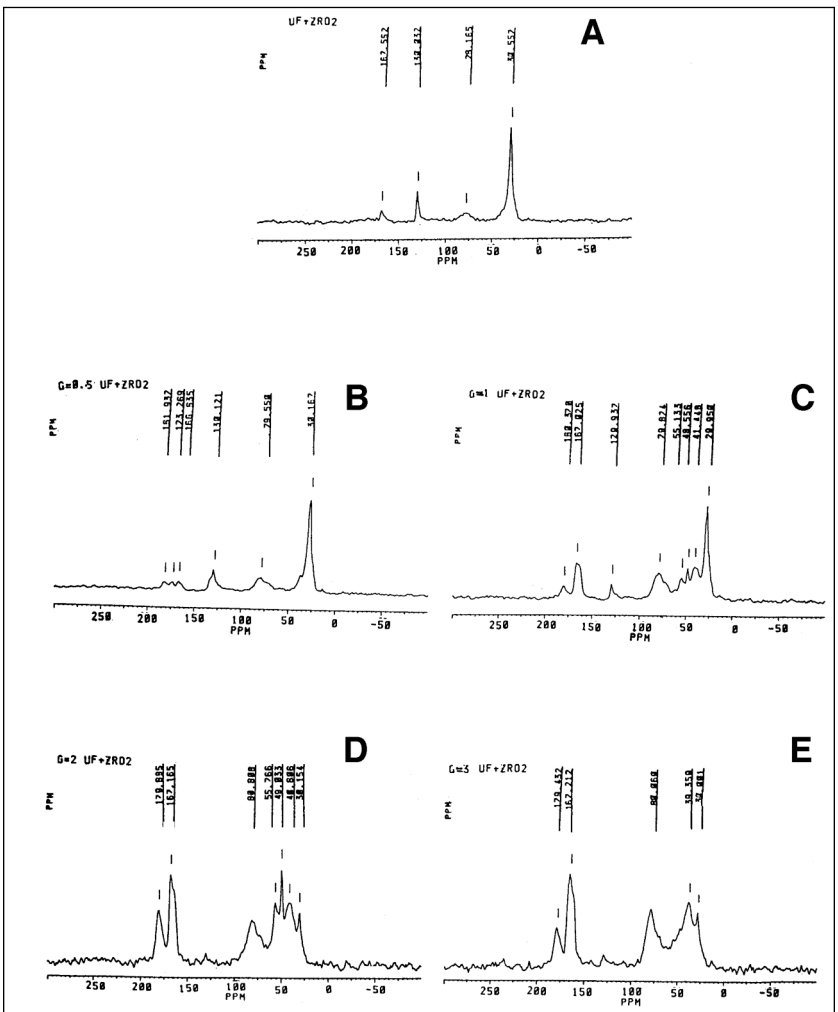

Figure 3. The solid-state ^{13}C NMR spectrograms of starburst dendritic spacer arms for (A) G = 0, (B) G = 0.5, (C) G = 1.0, (D) G = 2.0, and (E) G = 3.0.

In order to confirm the result of the coupling reaction, the active matrices of different generations (G = 0.5, 1.0, 2.0, and 3.0) were monitored by solid-state ^{13}C NMR, as shown in Figure 3. The ^{13}C CP MAS NMR experiments were performed on a Bruker AM 300 NMR spectrometer at a Larmor precession frequency of 75.47 MHz. The temperature was controlled at 296 K. The sample was packed into a 7-mm-diameter zirconia rotor. The contact time for cross polarization (CP) was 1.5 ms, a proton 90° pulse width was set at 5.1 µs, the number of scan was 3000, and the pulse repetition time was 3 s.The magic angle spinning (MAS) frequency was 4 KHz. For all spectra, the FID signal was accumulated in the 4-K data point. The external standard hexamethylbenzene was used for calibration of the ^{13}C scale.

Binding of the RNA ligand

RNA consists of multioligomers (polynucleotides) of AMP, uridine monophosphate, guanosine monophosphate (GMP), and cytidine monophosphate (19–22).

The position 8 active hydrogen atom located at the purine cyclo of AMP and GMP that is sited in

the chain elements of the RNA macromolecule can be substituted by bromine. When the RNA macromolecule is bromized, the chain elements of RNA can be cleft into the active 8-Br-RNA ligands with variable chain lengths. The 8-Br-RNA ligands can be further bonded to the amine end groups of starburst dendritic spacer arms on the composite microsphere matrix.

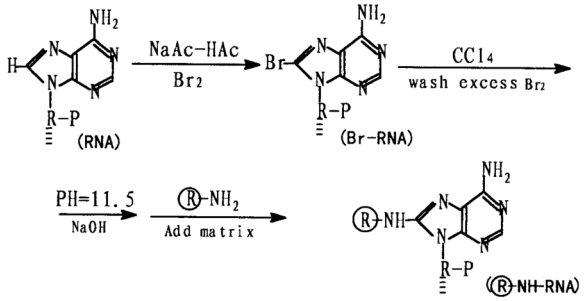

Figure 4. The bromating and binding process of RNA.

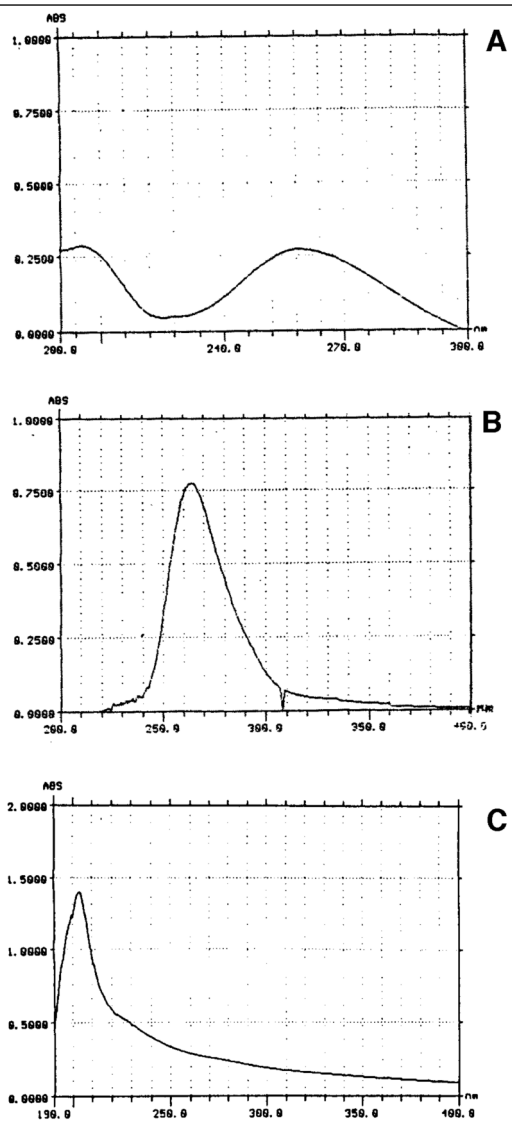

Figure 5. UV absorption spectrogram of (A) a standard RNA solution, (B) an HCl hydrolysate of RNA–(PAMAM)–(ZrO_2–UF resin), and (C) an HCL hydrolysate of (PAMAM)–(ZrO_2–UF resin) at G = 3.0.

The bromating and binding process can be produced in the following way (displayed in Figure 4). A 3.5-g sample of RNA is dissolved in 50 mL of a 0.5-mol/L sodium acetate buffer solution at pH 4.5 in a reaction vessel. Then, 3.0 mL of liquid bromine is added to the solution. The solution is vigorously stirred with a magnetic stirrer at room temperature for 2–4 h. The excess bromine in the reaction mixture is removed by repeating the extraction with carbon tetrachloride. The pH value of 8-Br-RNA ligands solution is adjusted from 9 to 11 by adding 0.1-mol/L sodium hydroxide. Then, approximately 2.0 to 2.5 g of composite microsphere matrix coupled with starburst dendritic spacer arms is added to the 8-Br-RNA ligands solution. The binding reaction is carried out for 48–96 h at room temperature under continuous stirring. The final reaction product is washed by a 0.5-mol/L sodium acetate buffer solution and deionized water until the pH is 7.0 in order to remove the adsorbed ligands. Consequently, the synthesized RNA–(PAMAM)–(zirconia–UF resin) stationary phase of HPLAC is obtained.

The binding capacity of the RNA ligand was measured by UV spectrophotometry and the results are shown in Figure 5.

Results and Discussion

Influence factors on the size of the composite microsphere particle

Influence of the surfactants

The sol-gel transition of zirconia generally occurs in a mixture of water and immiscible organic phase. Various nonionic surfactants were added into the mixture to stabilize the liquid–liquid dispersion. The stability of emulsion was adjusted by controlling the value of the hydrophilic–lipophilic balance (HLB) of the gelation reaction system. In this system, Span 80, Span 85, and Tween 80 with a certain ratio were selected as the emulsifier and mixed to get an emulsion possessing an HLB of 3.7. Under this condition, the emulsification efficiency and emulsion stability could reach the optimum state.

Influence of the initial concentration of reactants

The size of the particle was found to be very sensitive to the initial concentration of zirconyl chloride, HMTA, and urea. With the decreasing of the initial concentration of reactants, the size of the particle was gradually diminished. The result is shown in Table II.

Influence of stirring velocity

When the W/O emulsions were accomplished by the use of a high-speed stirrer, the generated small droplets were well-dispersed within the oil phase. The size of the droplet depended on the stirring velocity. Therefore, the particle size of the composite microsphere was decided. When the stirring velocity is more rapid, the size of the composite microsphere obtained becomes smaller.

Influence of the dropping velocity of zirconyl chloride

It was proved that the quicker the dropping velocity of zirconyl chloride, the bigger the particle size of composite microsphere (described in Table III).

Inspection of the solid-state ^{13}C NMR spectrogram of starburst dendritic spacer arms

Up to the present time, a solid-state ^{13}C NMR spectroscope with CP and MAS has been widely used for the investigation of a chemical-bonded stationary phase, polymer, biomacromolecule, and fossil fuels. The solid-state NMR provides important information on the molecular surface structure, and the chemical shift values found in the solid state are in good agreement with those measured in solution. The precision of solid-state NMR is lower than the liquid-state NMR. Therefore, the data obtained by solid-state ^{13}C NMR are relatively rougher.

The liquid-state ^{13}C NMR spectrogram of liquid PAMAM dendrimer has served as the best method for appraising branch characterization, as shown in reference 17.

The solid-state ^{13}C NMR spectrograms of starburst dendritic spacer arms coupled with the matrix of the composite microsphere of different generations (G = 0, 0.5, 1.0, 2.0, and 3.0) are shown in Figure 3. ^{13}C spectral data with assignments for starburst dendritic spacer arms (core = UF and G = 0.5, 1.0, 2.0, and 3.0) are shown in Table IV.

Starburst dendritic spacer arms that are successfully coupling on the matrix can be confirmed by two characteristic chemical

Table II. Effect of the Concentration of Reactant in the Oil Phase on the Diameter of Composite Microspheres

Zirconyl chloride (mol/L)	Urea (mol/L)	HMTA (mol/L)	Diameter (μm)
0.294	0.137	0.355	10–15
0.209	0.094	0.245	7–8
0.105	0.047	0.123	3–5

Table III. Effects of the Rate of Zirconyl Chloride Addition on the Diameter of Composite Microspheres

Rate of zirconyl chloride addition (mL/s)	Diameter (μm)
0.01667	15
0.01	7–8
0.0067	3–5

Table IV. ^{13}C Chemical Shift Assignments for Starburst Dendritic Spacer Arms

G	Structure	Assignment
Core (UF)	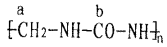	(a) 30.557 (b) 167.552
0.5	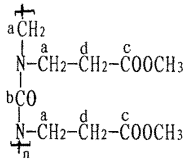	(a) 30.167 (b) 166.535 (c) 173.769 and 181.932 (d) 30.167 (OCH_3)
1.0	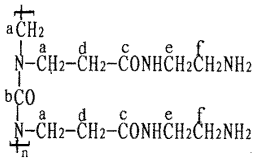	(a) 29.950 (b) 167.025 (c) 180.370 (d) 41.448 (e) 55.133 (f) 48.556
2.0	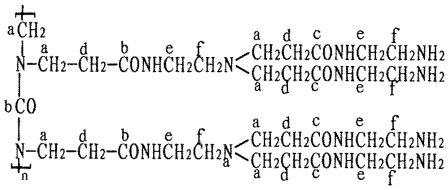	(a) 30.154 (b) 167.165 (c) 179.895 (d) 40.806 and 55.766 (e) 49.033
3.0	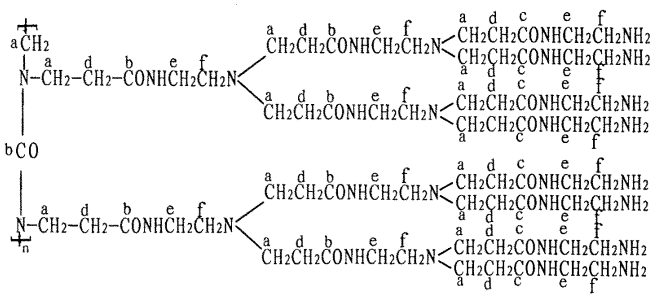	(a) 30.001 (b) 167.212 (c) 179.432 (d) 39.359 (e) 39.359 (f) 39.359

shifts in the spectrograms previously stated. One is the carbon of carbonyl groups appearing in the range of chemical shift at approximately 167. When the G increases, the content of carbonyl groups also rises. The chemical shift of carbon in carbonyl groups sited in the different positions of dendritic spacer arms resulting from the multigeneration array appeared near 167. This cannot indicate the precise difference of construction. Another is the carbon of methylene that bonds with -NH^- and -CO^- whose chemical shift displays in the 30- to 50-ppm range. When the generation numbers of dendrimer increases, more and more methylene forms are in the process of the branching of dendritic spacer arms. Therefore, the multipeaks can be found in the 30- and 50-ppm range.

The chemical shift of approximately 130 ppm is indicative of the carbon of –N=C=, which is the side product in the formation process of UF resin. The intensity of resonance at 130 ppm appears gradually in contraction with increasing generation numbers.

The signal at 80 ppm corresponds with some products of the unwanted side reaction such as the retro-Michael reaction, the intramolecular lactam formation in the amidation step, or both.

Determination of the binding capacity of the RNA ligand

The amount of RNA bonded on the active matrix was determined by UV absorption spectrophotometry. Figure 5A shows the UV absorption spectrogram of a standard RNA solution. It is well-known that a standard RNA solution produces a strong absorption peak at 260 nm.

When 0.25 g RNA–(PAMAM)–(ZrO_2-UF resin) stationary phase was added to 20 mL of a 0.5-mol/L HCl solution, the hydrolytic degradation reaction of the stationary phase occurred at 38°C with stirring maintained for 4 h. After centrifugal separation, the centrifugate was analyzed by UV spectrophotometry. The adsorption spectrogram of the RNA that was bonded on the active matrix is indicated in Figure 5B.

It should be noted that the absorption peak at 260 nm in Figure 5B was not formed by the hydrolysis of PAMAM dendrimer. The (PAMAM)–(ZrO_2–UF resin) active matrix (G = 3.0) was hydrolyzed by a 0.5-mol/L HCl solution in the same condition. On the absorption spectrogram, the strong absorption peak at 260 nm did not appear (as shown in Figure 5C).

As indicated previously, it was proven that RNA ligands were bonded to the active matrix coupled dendritic spacer arms.

According to the UV absorption spectrogram, it can be calculated that the binding capacity of the RNA ligands was 1.662 g RNA per gram stationary phase.

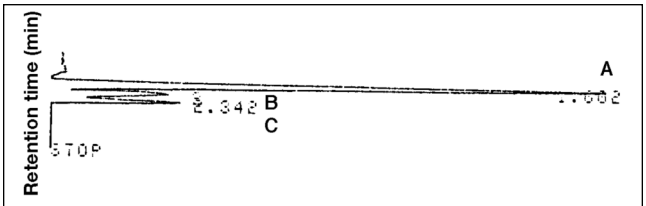

Figure 6. Separation of (A) AMP, (B) ADP, and (C) ATP. Chromatographic conditions: mobile phase = 0.025M NaH_2PO_4 and 0.025M Na_2HPO_4 buffer solution at pH 6.86, flow rate = 0.8 mL/min, sample injection = 3 µg, and λ for UVD = 254 nm.

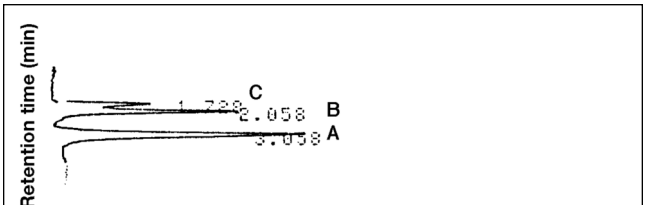

Figure 7. Purity analysis of bovine serum albumin (A) and two impurities (B and C). Chromatographic conditions: mobile phase = 20% methanol–80% acetonitrile, flow rate = 1.0 mL/min, sample injection = 5 µg, and λ for UVD = 280 nm.

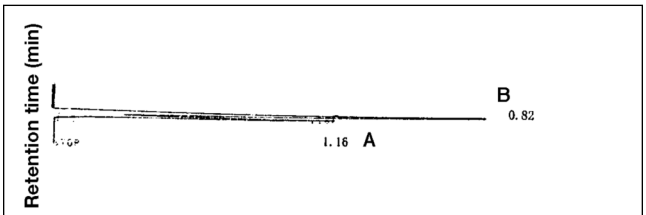

Figure 8. Separation of (A) cytochrome C and (B) cellulase. Chromatographic conditions: mobile phase = methanol, flow rate = 1.0 mL/min, sample injection = 2 µg, and λ for UVD = 280 nm.

Application of the new type of stationary phase in the analysis of biological macromolecules

The RNA–(PAMAM)–(ZrO_2–UF resin) stationary phase was packed into a 4.6-mm × 10-cm stainless steel column at 40 MPa by using a down-flow slurry packing method.

When the cellulase was used as the solute—an NaH_2PO_4–Na_2HPO_4 buffer solution (pH = 7.0) as the mobile phase using UVD—the column efficiency could reach more than 2×10^4 theoretical plates per meter column with the flow rate of 1.0 mL/min.

The new type of stationary phase was applied for the separation of AMP, ADP, and ATP (shown in Figure 6), the purity analysis of bovine serum albumin (shown in Figure 7), and the separation of cytochrome C and cellulase (shown in Figure 8) under different chromatographic analysis conditions.

Conclusion

A nonporous, monodisperse ZrO_2–UF resin composite microsphere (3–5 µm) was synthesized by means of a sol-gel conversion process and special particle processing procedures. The composite microsphere was used as the matrix of HPLAC and coupled with PAMAM starburst dendritic spacer arms by the multigeneration procedure in order to become the activated matrix. The activated matrix was bonded to the RNA ligand by the substitute reaction. As a result, a new type of HPLAC stationary phase was obtained.

The new type of stationary phase possessed three features. The first was a nonporous, rigid composite microsphere matrix; the second was starburst dendritic spacer arms; and the third was the RNA ligand possessing a molecular recognition ability.

For the separation of a biological macromolecule, the stationary phase that shows fast mass transfer, high column capacity, and strong specific biological recognition ability was preliminarily applied to the separation of nucleotide and the same protein. It is worth noticing that the stationary phase will show a more pow-

erful separation ability for the protein-bonded nucleic acids and peptide nucleic acids.

Acknowledgments

This work was financially supported by the National Natural Science Foundation of China (NNSFC). All of the authors express their deepest thanks.

References

1. K. Jones. New directions in affinity chromatography. *Anal. Proceedings* **30(2):** 78–79 (1993).
2. A. Lundqvist and P. Lundehl. Chromatography on cell and biomolecular assemblies. *J. Chromatogr. B* **699:** 209–20 (1997).
3. Y. Shibasawa. Surface affinity chromatography of human peripheral blood cells. *J. Chromatogr. B* **722:** 71–88 (1999).
4. K. Sproule, P. Morrill, J.C. Pearson, S.J. Burton, K.R. Hejnas, H. Valore, S. Ludvigsen, and C.R. Lowe. New strategy for the design of ligands for the purification of pharmaceutical proteins by affinity chromatography. *J. Chromatogr. B* **740:** 17–33 (2000).
5. S. Ohlson, L. Hansson, P.-O. Larsson, and K. Mosbach. High performance liquid affinity chromatography (HPLAC) and its application to the separation of enzymes and antigens. *FEBS Letters* **93(1):** 5–9 (1978).
6. F. Honda, H. Honda, and M. Koishi. Application of non-porous silica ultramicrospheres to high performance liquid chromatographic column packings. *J. Chromatogr.* **609:** 49–59 (1992).
7. W.-C. Lee, C.-H. Lin, R.-C. Ruaan, and K.-Y. Hsu. High performance affinity chromatography of proteins on non-porous polystyrene beads. *J. Chromatogr. A* **703:** 307–14 (1995).
8. J. Yu and Z. El Rassi. High performance liquid chromatography of small and large molecules with non-porous silica-based stationary phase. *J. Liq. Chrom. & Rel. Technol.* **20(2):** 183–201 (1997).
9. M. Leonard. New packing materials for protein chromatography. *J. Chromatogr. B* **699:** 3–27 (1997).
10. T. Issaeva, A. Kourganor, and K. Unger. Super-high-speed liquid chromatography of proteins and peptides on non-porous Micro NPS-RP packings. *J. Chromatogr. A* **846:** 13–23 (1999).
11. W.-C. Lee and C.-Y. Chuang. Performance of pH elution in high performance affinity chromatography of protein using non-porous silica. *J. Chromatogr. A* **721:** 31–39 (1996).
12. M. Hanson and K.K. Unger. Evaluation of advanced silica packing, Part I. Synthesis and charactrization of non-porous silica particles for HPLC. *LC-GC Int.* **10:** 650–56 (1996).
13. M. Hanson and K.K. Unger. Evaluation of advanced silica packing, Part II. Application of non-porous silica particles in HPLC. *LC-GC Int.* **11:** 741–46 (1996).
14. W.-C. Lee. Protein separation using non-porous sorbents. *J. Chromatogr. B* **699:** 29–45 (1997).
15. U. Trudinger, G. Muller, and K.K. Unger. Porous zirconia and titania as packing materials for high performance liquid chromatography. *J. Chromatogr.* **535:** 111–25 (1990).
16. D.A. Tomalia, H. Baker, J. Dewald, M. Hall, G. Kallos, S. Martin, J. Roeck, J. Ryder, and P. Smith. A new class of polymer: starburst-dendritic macromolecules. *Polymer J.* **17(1):** 117–32 (1985).
17. D.A. Tomalia, H. Baker, J. Dewald, M. Hall, G. Kallos, S. Martin, J. Roeck, J. Ryder, and P. Smith. Dendritic macromolecules: synthesis of starburst dendrimers. *Macromolecules* **19:** 2466–68 (1986).
18. D.A.Tomalia, A.M. Naylor, and W.A. Goddard, III. Starburst dendrimers: molecular-level control of size, shape, surface chemistry, topology, and flexibility from atoms to macroscopic matter. *Angew. Chem. Int. Ed. Engl.* **29:** 138–75 (1990).
19. L.B. McGown, M.J. Jeseph, J.B. Pitner, G.P. Vonk, and C.P. Linn. The nucleic acid ligand—a new tool for molecular recognition. *Anal. Chem.* **67(21):** 663A–68A (1995).
20. H.W. Jerrett. Affinity chromatography with nucleic acid polymer. *J. Chromatogr.* **618:** 315–39 (1993).
21. C.-Y. Lee and N.O. Kaplan. Characteristics of 8-substituted adenine nucleotide derivatives utilized in affinity chromatography. *Arch. Biochem. Biophys.* **168:** 665–76 (1975).
22. M.I. Shtilman. "Immobilization on Polymers". In *Nucleic Acids and Their Components*. VSP Utrecht, Tokyo, Japan, 1993, pp. 137–94.

Manuscript accepted March 23, 2001.